David Tomás Sánchez Martínez
Lourdes García Rodríguez
(coordinadores)

Proceedings of the 7th International Seminar on ORC Power Systems

Editorial Universidad de Sevilla

Proceedings of the 7th International Seminar on

ORC Power Systems

David Tomás Sánchez Martínez
Lourdes García Rodríguez
(coordinadores)

Proceedings of the 7th International Seminar on

ORC Power Systems

(ORC2023)

4th to 6th
SEPTEMBER
SEVILLE 2023

EDITORIAL UNIVERSIDAD DE SEVILLA

Sevilla, 2024

Colección Actas
Núm.: 91

Review chairs of the 7th International Seminar on ORC Power Systems

Prof. Christoph Wieland (University of Duisburg-Essen) - *Review Chair*
Prof. Sotirios Karellas (National Technical University of Athens) - *Review Co-Chair*
Prof. Teemu Turunen-Saaresti (LUT University) - *Review Co-Chair*
Dr. Diego-César Alarcón-Padilla (Plataforma Solar de Almería - CIEMAT) - *Review Co-Chair*
Dr. Francesco Crespi (Universidad de Sevilla) - *Review Co-Chair*

ISBN 978-84-472-2745-7
DOI: https://dx.doi.org/10.12795/9788447227457

Diseño de cubierta y maquetación: los autores

INDEX OF CONTRIBUTIONS

DOI: https://dx.doi.org/10.12795/9788447227457_17

Optimizing the performance of a hybrid Solar-Biomass micro-CHP system with a TFC engine as the prime mover for domestic applications

Anastasios Skiadopoulos[1,*], Xander van Heule[2], Steven Lecompte[2], Michel De Paepe[2], Dimitrios Manolakos

[1] *Agricultural University of Athens, Department of Natural Resources and Agricultural Engineering, Athens, Attica, Greece*
[2] *Ghent University, Department of Electromechanical, Systems and Metal Engineering, Ghent, Belgium*

*Corresponding Author: tskiado@aua.gr

ABSTRACT

The annual performance of a hybrid micro-Cogeneration of Heat and Power (CHP) system driven by solar energy and biomass with a Trilateral Flash Cycle (TFC) engine as the prime mover is simulated and optimized in this work. The system is sized to meet the Space Heating (SH) demand of a typical multi-family building in Athens, Greece. Particular attention is paid to the challenging two-phase expansion phenomenon, the factor mainly affecting the efficiency of the TFC, under off-design and partial load conditions. Under optimized operating conditions, the average annual CHP efficiency, TFC thermal efficiency, and solar energy conversion efficiency were estimated to be 89.2%, 8.4%, and 4.3%, respectively. The TFC can cover 18% of the building's SH demand and 40% of its electricity demand, with the Levelized Cost of Electricity (LCOE) and Levelized Cost of Heat (LCOH) in the range of 0.21~0.28 €/kWh$_{el}$, and 0.065~0.087 €/kWh$_{th}$, respectively. Furthermore, PayBack Periods (PBP), between 15 and 25 years, can be anticipated, when current market energy prices are considered.

1 INTRODUCTION

CHP is a well-established alternative to the standard practice of segregated electricity and heat production, because of increased primary energy conversion efficiency, and lower GreenHouse Gas (GHG) emissions. Micro-CHP units typically have a nominal electric capacity lower than 50 kW$_{el}$. They are particularly suitable for the domestic sector, a major energy consumer and GHG emitter in the EU. Micro-CHP systems driven by Renewable Energy Sources (RES), and hybridized by combining intermittent and stable RES, can play a significant role in increasing the energy efficiency of buildings, while reducing substantially their carbon footprint.

In regions with low to middle latitudes, it is of particular interest to study the sustainability of hybrid micro-CHP systems driven by solar energy and biomass (currently the RES with the highest share in the EU). Biomass Boilers (BB) for residences typically operate at top temperatures of about 90~95°C. On the other hand, several types of solar thermal collectors have been developed, capable to provide heat at temperatures up to 400°C, but, for residential applications, the temperature of the heat source is limited to a maximum of 120~130°C. At such temperature ranges of the heat source, an efficient heat-to-power technological solution is the utilization of a bottoming power cycle (Padinger, Aigenbauer, and Schmidl 2019).

Among the commonly applied bottoming power cycles, the Organic Rankine Cycle (ORC) has certain advantages, such as the low maintenance cost, nearly unsupervised operation, and flexibility in the design (Tchanche *et al.* 2011), that render it a promising solution for residential micro-CHP. However, in an ORC, the potential of the heat source is not optimally exploited, because of the increased exergy losses during the evaporation of the WF in the evaporator (Schuster *et al.* 2010). The temperature of the finite heat source drops as the WF evaporates isothermally, leading to reduced attainable evaporating

pressure, and, consequently, generated power. This sub-optimal match between the heat source and the WF at the evaporator of an ORC can be overcome if the evaporation of the WF is omitted, transforming the power cycle into a triangle (Schuster *et al.* 2010).
A promising alternative to the ORC power cycle is the TFC, originally conceptualized for optimal heat recovery in geothermal applications (Smith 1993). In the TFC, the WF enters the suction port of the expansion machine in the saturated liquid state (or two-phase mixture in the generalization of the concept), where two-phase expansion, also known as flashing, occurs, and power is generated. Several theoretical studies comparing the TFC and the ORC for various heat sources (e.g. see (Fischer 2011)) have been published. They highlight the potential of the TFC as a high-efficiency alternative to the ORC. However, the technological maturity of the TFC is low because flashing is a complex non-equilibrium phenomenon, and the efficiency of expanders in the two-phase region is not sufficiently mapped. Only a handful of experimental works in flashing have been undertaken (Öhman and Lundqvist 2013; Smith, Stošić, and Aldis 1996), all indicating that the efficiency of two-phase expansion improves as the quality of the WF at the suction port of the expander increases.
The purpose of this work is to numerically assess the performance of a novel hybrid micro-CHP system in Athens, Greece, driven by solar energy and biomass, and a TFC engine as the prime mover. The unit consists of a BB, an array of Evacuated Tube Collectors (ETC), a TFC engine, with a twin-screw expander as the expansion machine, and a Thermal Energy Storage (TES) tank. It operates in heat-driven mode, and it is sized to meet the SH demand of an average-sized multi-family building. An integrated numerical tool is developed in Matlab to calculate the energy output of the micro-CHP system on an annual basis, with an hourly time step. A novel feature of this work is that the efficiency of two-phase expansion under off-design operating conditions is carefully monitored, by applying a dedicated thermodynamic low-order model (Skiadopoulos *et al.* 2021). Optimization simulations are performed pinpointing the operating conditions that maximize total efficiency on an annual basis. This study concludes with a preliminary economic analysis to assist in an initial assessment of the modeled system's competitiveness.

2 MODEL RESIDENCE

The model residence is a multi-family house in Athens, Greece, consisting of ten average-sized multi-family apartments, with a total floor area of 920 m^2, a shape factor equal to 1.1, and 10% openings coverage on its faces. The heating period is assumed to start on October 15 and end on April 15. The U values for the building's structural elements, extracted from the EU Buildings Database, are assumed to be average values of the buildings' inventory in Greece. The SH demand of the building is calculated on an hourly basis for the heating period, assuming a desired internal temperature of 20^{o}C and an operating temperature threshold of 15^{o}C for the heating system. Typical meteorological Year (TMY) data for Athens are taken from the PVGIS database. The annual electricity demand for the building is calculated utilizing average electricity consumption data for households in Greece, and it is assumed that the annual electricity demand is distributed uniformly throughout the year. The energy demand data for the model residence are listed in Table 1, where $\dot{Q}_{sh,max}$, $Q_{th,an}$, and $P_{el,an}$ are the maximum hourly SH demand, the total annual heating demand, and the total annual electricity demand of the building, respectively.

Table 1: Energy demand of model residence

$\dot{Q}_{sh,max}$ **[kW$_{th}$]**	$Q_{th,an}$ **[MWh$_{th}$]**	$P_{el,an}$ **[MWh$_{el}$]**
83.56	132.79	34.22

3 MICRO-CHP SYSTEM

Description

The layout of the modeled micro-CHP system is presented in Figure 1. Two different modes of operation are selected, i.e. a CHP mode, and a TFC mode. In CHP mode, the TFC operates when there is sufficient solar irradiance (over 400 W/m^2 for this work), and the condenser of the engine, with water as the Cooling Fluid (CF), charges the TES, which provides heat to the building. The BB acts as an

auxiliary heat source when the capacity of the TES is not sufficient. In TFC mode, only the TFC operates, and heat is dissipated in an air-cooled condenser.
When the system operates in CHP mode, the temperature of the Heat Transfer Fluid (HTF) at the system evaporator is in the range of 100~120ºC, whereas in the summer period, the respective range is 80~120ºC. Water pressurized at 4 bar, to avoid partial evaporation in the solar collectors' circuit, is selected as the HTF. The generated electricity from the TFC would, in an actual building, be, by priority, utilized to cover its energy demand, and the surplus could be sold to the power grid or stored locally. However, in this work, it is assumed that the generated electricity is used only to cover the building's demand, averaged on a monthly and annual basis, since an electricity demand profile, that would allow calculating the actual hourly surplus or deficit, is not available.

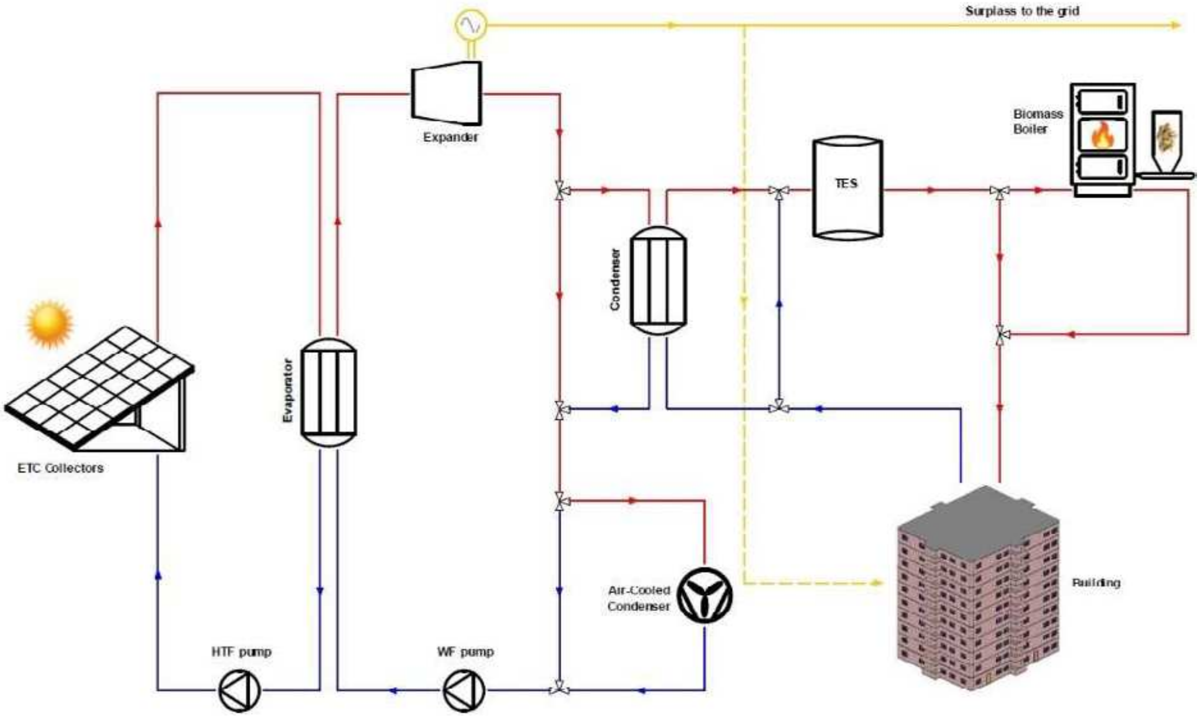

Figure 1: Layout of the hybrid micro-CHP system.

111

Components' sizing
The Thermomax DF 100 30 ETCs, developed by Thermomax Ltd., are selected as the solar field of the system. The area A_{col} of the collectors is equal to 180 m^2, indirectly estimated by calculating the necessary heat duty $\dot{Q}_{htf}$ (an equation for the calculation of the collectors' heat duty is given in Section 4) from the solar field at an average temperature of the HTF equal to 120ºC, ambient temperature T_{amb} equal to 20ºC, and solar irradiance normal on the ETCs 1000 W/m^2, while assuming a target thermal efficiency n_{th} equal to 10% for the TFC, and a heat duty $\dot{Q}_{con}$ at the condenser equal to $\dot{Q}_{sh,max}$. At these operating conditions, the nominal electric capacity P_{tfc} of the TFC becomes equal to 10 kW$_{el}$.
The minimum and maximum allowed temperatures of water in the TES are assumed to be 45 and 50ºC, respectively. The necessary volume V_{TES} of the TES is 15 m^3, estimated assuming that the heat capacity of the TES should meet $\dot{Q}_{sh,max}$ within one hour. Finally, the nominal capacity $\dot{Q}_{BB,nom}$ of the BB is equal to 90 kW$_{th}$, sufficient to meet $\dot{Q}_{sh,max}$.

4 MODELING

Solar Field
The parameters of the ETCs are listed in Table 2, with η_o the optical efficiency at normal incidence, and a_1, a_2 the first and second order losses coefficient, respectively. The inclination angle

β is selected to maximize the solar irradiance normal on the collectors at the studied location on an annual basis.

Table 2: Solar field parameters

η_o [-]	a_1 [W/m^2-K]	a_2 [W/m^2-K^2]	β [°]
0.832	1.14	0.0144	32

Under steady-state operation of the ETCs, the heat transfer rate $\dot{Q}_{ev}$ from the ETCs to the HTF is given by Equation (1), where G_t is the total irradiance on the collectors. Moreover, $\dot{m}_{htf}$ and $c_{p,ht}$ are the mass flow rate and the specific heat, under constant pressure, of the HTF, respectively. Finally, $T_{htf,out}$ and $T_{htf,in}$ are the temperatures of the HTF flowing in and out of the ETCs, respectively.

$$\dot{Q}_{ev} = A_{col} \cdot [G_t \cdot \eta_o - a_1 \cdot (T_m - T_{amb}) - a_2 \cdot (T_m - T_{amb})^2] = \\ = \dot{m}_{htf} \cdot c_{p,htf}(T_{htf,out} - T_{htf,in}) \quad (1)$$

The efficiency η_{col} of the ETCs is given by Equation (2).

$$\eta_{col} = \eta_o - a_1 \cdot (T_m - T_{amb})/G_t - a_2 \cdot (T_m - T_{amb})^2/G_t = \dot{Q}_{ev}/(A_{col} \cdot G_t) \quad (2)$$

TFC

Assuming negligible heat losses at the evaporator, $\dot{Q}_{ev}$ will also be equal to the heat transfer rate from the HTF to the WF. This assumption is expressed by Equation (3), where $\dot{m}_{wf}$ is the mass flow rate of the WF, while $h_{ev,in}$ and $h_{ev,out}$ are its specific enthalpies at the inlet and outlet of the evaporator, respectively.

$$\dot{Q}_{ev} = \dot{m}_{wf} \cdot (h_{ev,out} - h_{ev,in}) \quad (3)$$

The condensation temperature T_{con} of the WF is given by Equation (4), where $T_{cf,out}$ is the temperature of the CF at the outlet of the evaporator, and PP_{con} the pinch-point temperature difference at the condenser. When the CF is Air, $T_{cf,out}$ is equal to $T_{amb} + \Delta T_{CF}$, with ΔT_{CF} denoting the allowed temperature rise of the CF. When the TFC operates in CHP mode, $T_{cf,out}$ is equal to the temperature T_{TES} of water in the TES at the beginning of the timestep. The determination of T_{con} leads directly to the calculation of the condensation pressure p_{con}. 112

$$T_{con} = T_{cf,out} + PP_{con} \quad (4)$$

The coupling between the TFC and the ETCs at the evaporator is accomplished by the pinch point temperature difference PP_{ev} in an iterative manner. Specifically, Equations (3),(5), and (6) are solved iteratively until convergence, with $\dot{m}_{wf}$, and the evaporation pressure p_{ev}, the iteration variables for a given quality $x_{ex,in}$ of the WF at the suction port of the expander. In Equation (5) $T_{htf,pr}$ is the temperature of the HTF at the end of preheating. In Equation (6), $\dot{Q}_{pr}$ denotes the heat transfer rate to the WF during preheating.

$$T_{htf,pr} = T_{sat,wf}(p_{ev}) + PP_{ev} \quad (5)$$

$$\dot{Q}_{pr} = \dot{m}_{wf} \cdot (h_{l,sat}(p_{ev}) - h_2) = \dot{m}_{htf} \cdot c_{p,htf} \cdot (T_{htf,pr} - T_{htf,in}) \quad (6)$$

Having calculated $\dot{m}_{wf}$ and p_{ev}, the thermodynamic low-order model simulating two-phase expansion (Skiadopoulos *et al.* 2021) in the twin-screw expander is applied to calculate the specific enthalpy $h_{con,in}$ of the WF at the expander's discharge. The power $\dot{w}_{ex}$ generated by the expander is given by Equation (7), where $\eta_{ex,is}$ is the isentropic efficiency of the expander, and $h_{con,in,is}$ is the WF's specific enthalpy corresponding to an isentropic expansion to p_{con}.

$$\dot{w}_{ex} = \dot{m}_{wf} \cdot (h_{ev,out} - h_{con,in}) = \dot{m}_{wf} \cdot \eta_{ex,is} \cdot (h_{ev,out} - h_{con,in,is}) \quad (7)$$

The required power $\dot{w}_{pu,tfc}$ from the TFC pump is given by Equation (8), where $\eta_{pu,is}$ is the pump's isentropic efficiency, and $h_{ev,in,is}$ the specific enthalpy of the WF corresponding to an isentropic pumping to p_{ev}.

$$\dot{w}_{pu,tfc} = \dot{m}_{wf} \cdot (h_{ev,in} - h_{con,out}) = \dot{m}_{wf} \cdot (h_{ev,in,is} - h_{con,out})/\eta_{pu,is} \quad (8)$$

The heat rate $\dot{Q}_{con}$ at the condenser is given by Equation (9), with $h_{con,out}$ the specific enthalpy of the WF at the outlet of the condenser.

$$\dot{Q}_{con} = \dot{m}_{wf} \cdot (h_{con,out} - h_{con,in}) \quad (9)$$

The thermal efficiency η_{th} of the TFC is calculated by Equation (10), where $\dot{w}_{pu,htf}$ denotes the power absorbed by the HTF pump.

$$\eta_{th} = \dot{w}_{net}/\dot{Q}_{ev} = \left(\dot{w}_{ex} - \dot{w}_{pu,tfc} - \dot{w}_{pu,htf}\right)/\dot{Q}_{ev} \tag{10}$$

Table 3: Modeling parameters of the TFC cycle

PP_{ev} [ºC]	PP_{con} [ºC]	$\eta_{pu,is}$ [-]	WF [-]	CF [-]	$\eta_{pu,htf}$ [-]	ΔT_{sub} [ºC]	ΔT_{CF} [ºC]
5	5	0.75	R245fa	Water & Air	0.70	5	10

The values of the TFC modeling parameters are compiled in Table 3. The values of the parameters are typical in power cycle modeling, and a sensitivity analysis, beyond the purpose of this work, should be undertaken to highlight their effect on the performance of the TFC. ΔT_{sub} and $\eta_{pu,ht}$ are the total efficiency of the HTF pump, and the WF sub-cooling at the pump suction, respectively.

TES

The energy balance of the TES is expressed by Equation (11), where ΔT_{TES} is the temperature difference of water in the TES, and $\dot{Q}_{sh,TES}$ the heat rate from the TES to the building for SH purposes. Moreover, Δt_{CHP} is the time step for the simulations of the micro-CHP system, equal to 1 hr. Finally, $m_{H_2O,TES}$ and $c_{p,H_2O,TES}$ are the total mass and the specific heat of water in the TES, respectively.

$$m_{H_2O,TES} \cdot c_{p,H_2O,TES} \cdot (\Delta T_{TES}/\Delta t_{CHP}) = \dot{Q}_{con} - \dot{Q}_{sh,TES} \tag{11}$$

It must be noted that thermal losses from the TES to the ambient are neglected for this work.

CHP

The total SH demand $\dot{Q}_{sh}$ of the building within Δt_{CHP} is calculated by Equation (12), where $\dot{Q}_{sh,BB}$ is the heat rate from the BB.

$$\dot{Q}_{sh} = \dot{Q}_{sh,TES} + \dot{Q}_{sh,BB} \tag{12}$$

By priority, $\dot{Q}_{sh}$ is covered by the TES. If its heat capacity is not sufficient at the beginning of the timestep, the BB acts as an auxiliary heat source.

Performance indices

The total solar energy conversion efficiency is given by Equation (13),

$$\eta_{tot,sol} = \eta_{col} \cdot \eta_{th} = \dot{w}_{net}/(A_{col} \cdot G_t) \tag{13}$$

whereas the CHP efficiency η_{CHP} is calculated by Equation (14), where η_{BB} is the efficiency of the BB, taken equal to 85% in this work.

$$\eta_{CHP} = \frac{\dot{w}_{net} + \dot{Q}_{con}}{\dot{Q}_{ev} + \dot{Q}_{sh,BB}/\eta_{BB}} \tag{14}$$

Economic analysis

The capital investment C_{inv} is calculated by Equation (15),

$$C_{inv} = sc_{tfc} \cdot P_{tfc} + sc_{col} \cdot A_{col} + sc_{BB} \cdot \dot{Q}_{BB,nom} + C_{TES} \tag{15}$$

where sc_{tfc}, sc_{col}, and sc_{BB} are the specific investment costs for the TFC, the ETCs, and the BB, respectively. Moreover, C_{TES} is the investment cost for the TES, given by Equation (16) (González-Pino *et al.* 2020).

$$C_{TES} = 29.968 \cdot {V_{TES}}^{0.6382} \tag{16}$$

The $LCOE$ and $LCOH$, and PBP, given by Equations (17), (18), and (19), respectively, indices are utilized for a preliminary economics analysis. In Equations (17), (18), and (19) cw_{el} and cw_{th} represent the contribution of electricity and heat to the total cost of the micro-CHP system over its lifetime N_{lt}. Also, e_{el} and e_{he} denote the price of electricity and heating, respectively, for households in Greece. Moreover, E_{tot} and Q_{tot} are the total electricity and heat produced annually by the unit (considered constant over N_{lt}). Finally, C_{fuel} is the total cost of biomass for the operation of the system in a year, M the, constant, annual maintenance cost, and r is the interest rate. The values of the economic analysis parameters are listed in Table 4.

$$LCOE = cw_{el} \cdot \left(C_{inv} + \sum_{i=1}^{N_{lt}} \frac{M + C_{fuel}}{(1+i)^r} \right) \Bigg/ \sum_{i=1}^{N_{lt}} E_{tot} \tag{17}$$

$$LCOH = cw_{th} \cdot \left(C_{inv} + \sum_{i=1}^{N_{lt}} \frac{M + C_{fuel}}{(1+i)^r} \right) \Bigg/ \sum_{i=1}^{N_{lt}} Q_{tot} \tag{18}$$

$$PBP = \frac{C_{inv}}{E_{tot} \cdot e_{el} + Q_{tot} \cdot e_{he} - \left(M + C_{fuel}\right)} \tag{19}$$

Table 4: Parameters of the economic analysis

sc_{tfc} [€/kW$_{el}$]	sc_{col} [€/m^2]	sc_{BB} [€/kW$_{th}$]	N_{lt} [yr]	r [%]	M [€]	cw_{el} [-]	cw_{th}[-]
2000~4000	200~400	900~1200	20	5	$0.01 \cdot C_{inv}$	0.25	0.75

5 RESULTS & DISCUSSION

The hybrid micro-CHP system's governing equations, along with the ones of the thermodynamic low-order two-phase expansion model (Skiadopoulos *et al.* 2021), are integrated into a numerical model in the software environment of Matlab (R2022b). Three operational degrees of freedom are identified, i.e. T_m, $x_{ex,in}$ and $\dot{m}_{htf}$, by inspecting the governing equations. The target of the simulations is to maximize total efficiency at the current timestep, and not the optimization of the TFC sub-system. This implies that the TFC will operate at off-design and partial load conditions for long periods during the year. As a result, another primary target of this study is accomplished, which is the monitoring of the efficiency of the TFC under varying operating conditions. The performance optimization of the hybrid micro-CHP system is performed within Matlab, by applying a native genetic optimization algorithm, with T_m, $x_{ex,in}$ and $\dot{m}_{htf}$ constituting the optimization parameters. When the system operates in CHP mode, the target is to maximize η_{CHP}, otherwise, the target of the simulations is to maximize $\eta_{tot,sol}$.

TFC

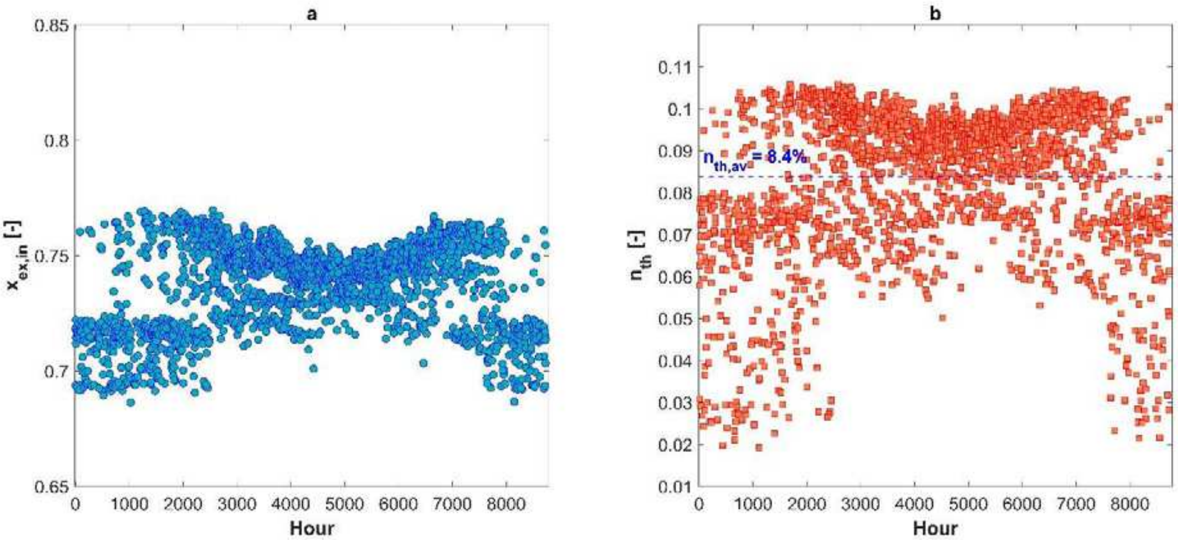

Figure 2: a) Optimal $x_{ex,in}$ and b) η_{th} of the TFC over the year.

The optimal values of $x_{ex,in}$, and the obtained η_{th} of the TFC throughout the year are presented in Figure 2. Higher values of $x_{ex,in}$ maximize the efficiency of the TFC, because $\eta_{ex,is}$ improves as the amount of vapor at the suction port of the expander increases. Concerning η_{th}, values as high as 10.5% can be achieved, with an annual average $\eta_{th,av}$ equal to 8.4%. The estimated values for $\eta_{th,av}$ and maximum η_{th} are within the range documented in the literature (7.5-13%) for micro-CHP systems with the ORC as the prime mover (González *et al.* 2015). However, a concrete conclusion concerning the competitiveness of the TFC against the ORC for micro-CHP systems will be reached when the two technologies are compared under the same operating conditions.

Micro-CHP Performance

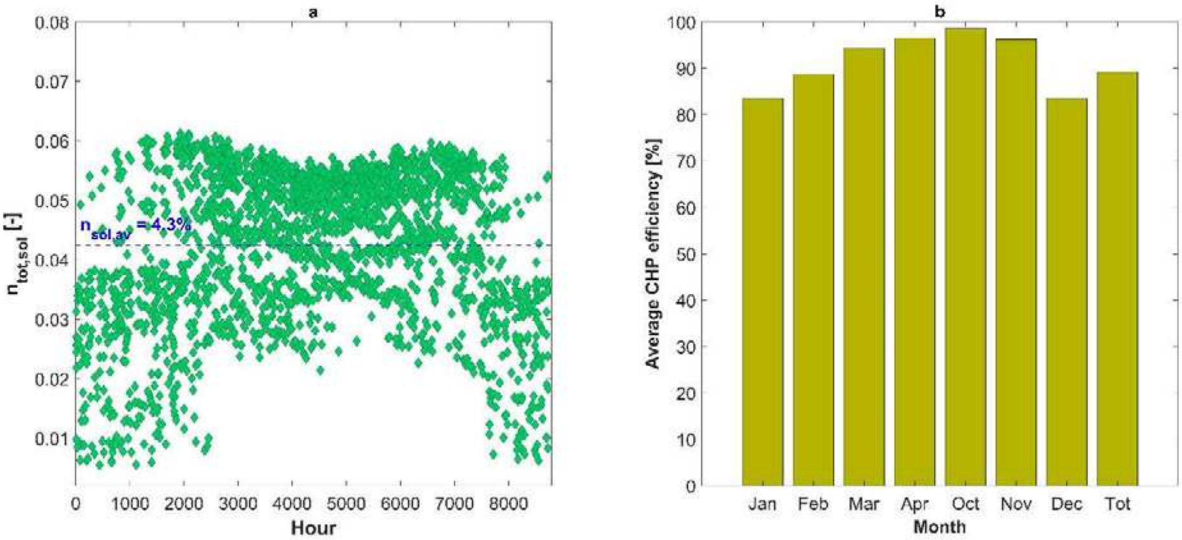

Figure 3: a) $\eta_{tot,sol}$ over the year, and b) Average monthly and annual η_{CHP}.

The TFC and BB will operate in Athens for 2344 and 2495 hours, respectively. The values of $\eta_{tot,sol}$ throughout the year, along with the average monthly and annual η_{CHP} are presented in Figure 3. The Solar-TFC subsystem of the micro-CHP can achieve an annual average value for $\eta_{tot,sol}$ equal to 4.3%, higher than the one estimated (3%) for a small-scale Solar-ORC system in Athens with similar architecture (Soulis *et al.* 2022). The average η_{CHP} over the heating period is equal to 89.2%, with higher values observed as the BB's contribution is decreased. The η_{CHP} values estimated herein are substantially higher than the ones reported for micro-CHP systems driven by an ORC (60-80%) (González *et al.* 2015). However, it must be mentioned that no heat losses toward the ambient, or pressure losses in the hydraulic circuits have been considered in the present work. 115

The monthly and annual contributions of the TFC and BB in the coverage of the building's SH demand, along with the contribution of the TFC in the electricity demand, are presented in Figure 4. The TFC can cover approximately 18% of the SH demand and 40% of the electricity demand over the year, highlighting the added value coming from the flexibility to operate the unit in TFC mode.

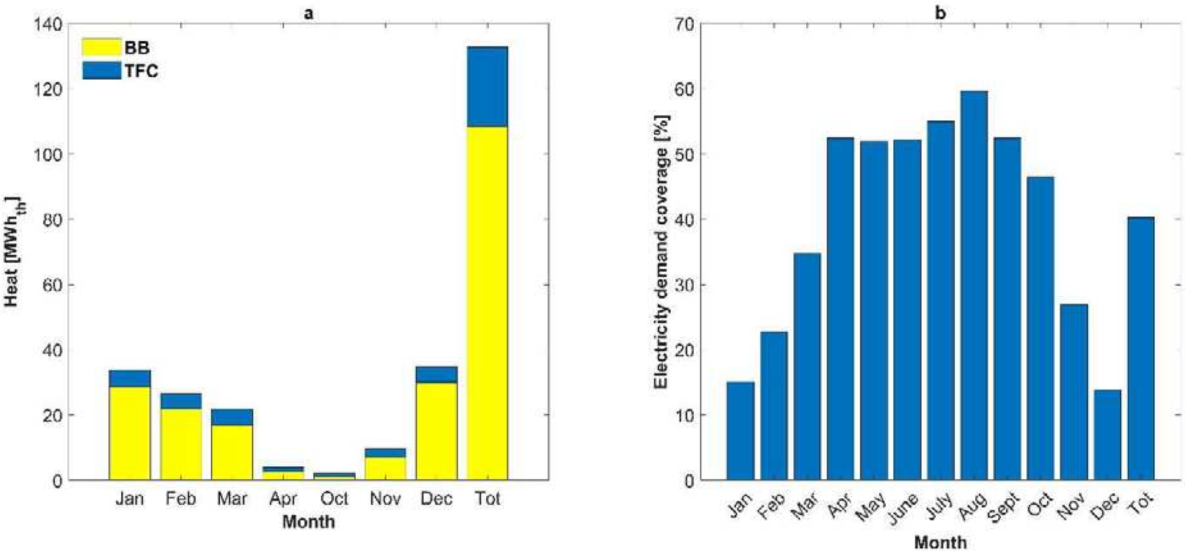

Figure 4: Monthly and annual contribution of a) the TFC and the BB in the coverage of the SH demand, and b) the TFC in electricity demand coverage of the building.

Economic assessment

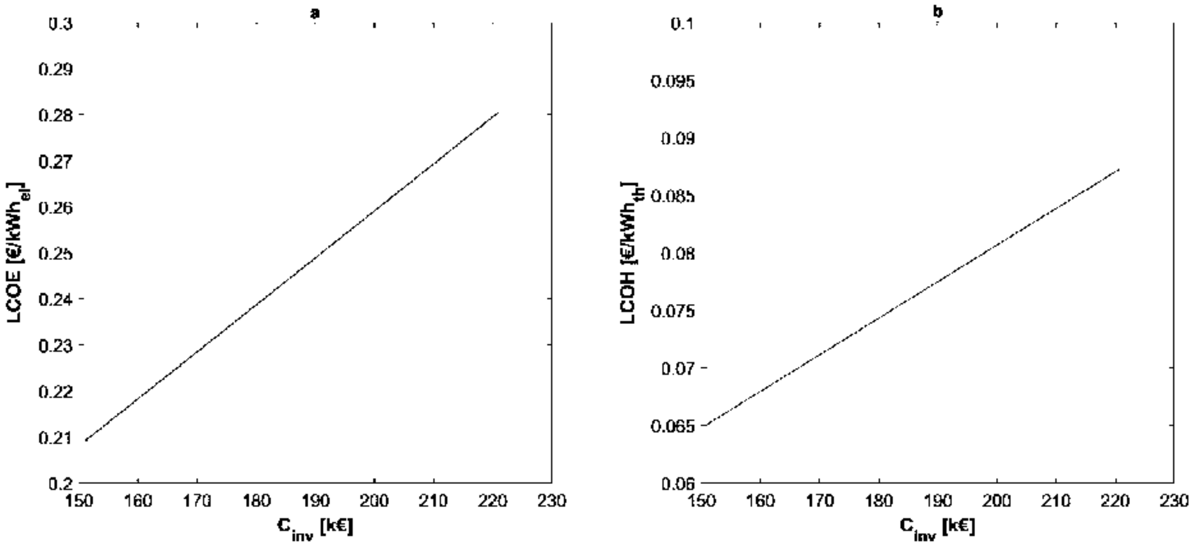

Figure 5: a) $LCOE$, and b) $LCOH$ as a function of C_{inv}.

A parametric economic assessment of the micro-CHP system is performed, with C_{inv} the parameter. For this purpose, the upper and lower limits of C_{inv} are calculated, based on the ranges of sc_{tfc}, sc_{col}, and sc_{BB} in Table 4. For the estimation of C_{fuel}, wood pellets, with a lower heating value of 4.9 kWh/kg, and an average market price of 0.22€/kg, are considered. It is reckoned that approximately 22 tons of wood pellets are required to operate the micro-CHP system annually. It must be stressed that in a more elaborate economic analysis, the effect of the type and market price of biofuel must be considered.

The values of $LCOE$ and $LCOH$ as a function of C_{inv} are plotted in Figure 5. Competitive values for heating and electricity are estimated, considering their current market prices in the EU, and the uncertainty in the price and availability of fossil fuels. These values can be further diminished by decreasing the specific investment costs of the equipment and by introducing financial incentives to assist the penetration of RES in the energy mix.

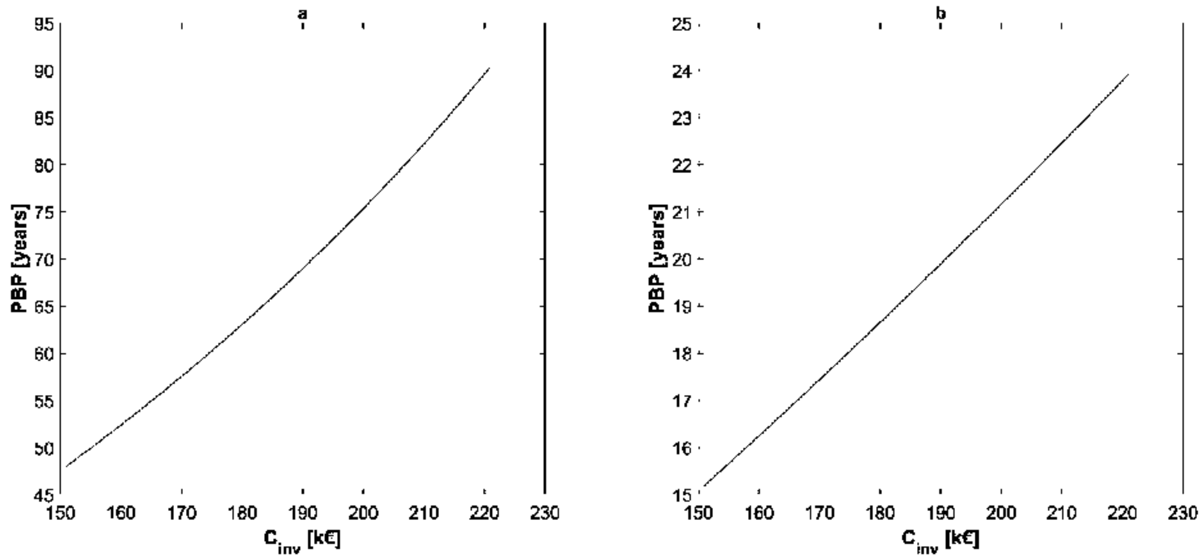

Figure 6: PBP for a) EU-27 average e_{el} and e_{he} prices in 2nd half of 2021, and b) EU-27 average e_{el} and e_{he} prices in 2nd half of 2022, as a function of C_{inv}.

For the estimation of PBP, it is assumed that e_{he} is equal to the price of natural gas that would be used for SH in the model residence if the micro-CHP unit was not installed. On the other hand, e_{el} is equal to the electricity price of the power grid. Two different cases are examined for e_{el} and e_{he} to illustrate the sensitivity of PBP on market prices of energy. In the first scenario, e_{el} and e_{he} are equal to the average price of electricity and natural gas for the EU-27 in the second half of 2021 (e_{el}= 0.13 €/kWh$_{el}$ and e_{he}= 0.06 €/kWh$_{th}$), whereas, in the second scenario, the respective values for the second half of 2022 are considered (e_{el}= 0.24 €/kWh$_{el}$ and e_{he}= 0.10 €/kWh$_{th}$). PBP as a function of C_{inv} for the two examined cases is plotted in Figure 6. Favorable values are obtained for PBP when the current energy market prices are considered. However, if these prices drop substantially in the future, the economic viability of the modeled micro-CHP unit will be based on the reduction of C_{inv} and the concurrent quest for more economical biofuels.

6 CONCLUSIONS

In the present work, the annual performance of a hybrid micro-CHP system with a TFC engine as the prime mover was simulated. The system is driven by solar energy and biomass, and it was sized to meet the annual SH demand of an average-sized multi-family building in Athens, Greece. Optimization simulations were undertaken to maximize the primary energy conversion efficiency throughout the year for all the selected operational modes.

The numerical experiments indicated that the hybrid unit can achieve an average CHP efficiency of 89.2% over the heating period, with higher values observed as the contribution of solar energy to the building's energy mix increases. The TFC can cover 18% of the building's annual SH demand, and 40% of the annual electricity demand. The average annual solar energy conversion efficiency of the Solar-TFC subsystem reaches 4.3%, whereas the average annual, and maximum thermal efficiency of the TFC are 8.4% and 10.5%, respectively. In the simulations, particular attention was paid to the flashing phenomenon in the TFC expander, the main phenomenon affecting the TFC thermal efficiency, under varying operating conditions. It was pointed out that higher vapor qualities at the onset of two-phase expansion ensure optimal operation of the two-phase expander. Competitive values, compared to current market energy prices, of $LCOE$ (0.21~0.28 €/kWh$_{el}$) and $LCOH$ (0.065~0.087 €/kWh$_{th}$) were estimated. On the other hand, the PBP values are more favorable when current prices of electricity and heating for households are considered.

Concluding, it must be stressed that the presented herein model needs to be appended so that it can also model an ORC, to perform a detailed comparison between the TFC and the ORC as bottoming cycles for the modeled hybrid micro-CHP unit. This will be accomplished when the developed expander model is calibrated to model expansion in the dry vapor region as well. Also, different layouts, operational modes, and types of solar collectors must be examined, and the environmental impact of the unit has to be assessed.

REFERENCES

Fischer, Johann. 2011. "Comparison of Trilateral Cycles and Organic Rankine Cycles." *Energy* 36(10):6208–19. doi: 10.1016/J.ENERGY.2011.07.041.

González-Pino, I., E. Pérez-Iribarren, A. Campos-Celador, and J. Terés-Zubiaga. 2020. "Analysis of the Integration of Micro-Cogeneration Units in Space Heating and Domestic Hot Water Plants." *Energy* 200:117584. doi: 10.1016/J.ENERGY.2020.117584.

González, Arnau, Jordi Roger Riba, Rita Puig, and Pere Navarro. 2015. "Review of Micro- and Small-Scale Technologies to Produce Electricity and Heat from Mediterranean Forests' Wood Chips." *Renewable and Sustainable Energy Reviews* 43:143–55. doi: 10.1016/J.RSER.2014.11.013.

Öhman, Henrik, and Per Lundqvist. 2013. "Experimental Investigation of a Lysholm Turbine Operating with Superheated, Saturated and 2-Phase Inlet Conditions." Pp. 1211–18 in *Applied Thermal Engineering*. Vol. 50. Pergamon.

Padinger, Reinhard, Stefan Aigenbauer, and Christoph Schmidl. 2019. "Best Practise Report on Decentralized Biomass Fired CHP Plants and Status of Biomass Fired Small-and Micro Scale CHP Technologies."

Schuster, A., S. Karellas, and R. Aumann. 2010. "Efficiency Optimization Potential in Supercritical Organic Rankine Cycles." *Energy* 35(2):1033–39. doi: 10.1016/J.ENERGY.2009.06.019.

Skiadopoulos, Anastasios, Xander van Heule, George Kosmadakis, Dimitrios Manolakos, Michel de Paepe, and Steven Lecompte. 2021. "Thermodynamic Low-Order Model for the Simulation of

Two-Phase Expansion within a TFC Unit." in *Proceedings of the 6th International Seminar on ORC Power Systems*, edited by T. U. of Munich. Technical University of Munich.

Smith, I. K. 1993. "Development of the Trilateral Flash Cycle System: Part 1: Fundamental Considerations." *Proceedings of the Institution of Mechanical Engineers, Part A: Journal of Power and Energy* 207(3):179–94. doi: 10.1243/PIME_PROC_1993_207_032_02.

Smith, I. K., N. Stošić, and C. A. Aldis. 1996. "Development of the Trilateral Flash Cycle System. Part 3: The Design of High-Efficiency Two-Phase Screw Expanders." *Proceedings of the Institution of Mechanical Engineers, Part A: Journal of Power and Energy* 210(1):75–92. doi: 10.1243/pime_proc_1996_210_010_02.

Soulis, Konstantinos X., Dimitris Manolakos, Erika Ntavou, and George Kosmadakis. 2022. "A Geospatial Analysis Approach for the Operational Assessment of Solar ORC Systems. Case Study: Performance Evaluation of a Two-Stage Solar ORC Engine in Greece." *Renewable Energy* 181:116–28. doi: 10.1016/J.RENENE.2021.09.046.

Tchanche, Bertrand F., Gr Lambrinos, A. Frangoudakis, and G. Papadakis. 2011. "Low-Grade Heat Conversion into Power Using Organic Rankine Cycles - A Review of Various Applications." *Renewable and Sustainable Energy Reviews* 15(8):3963–79. doi: 10.1016/J.RSER.2011.07.024.

ACKNOWLEDGEMENT

The research work was supported by the Hellenic Foundation for Research and Innovation (H.F.R.I.) under the "First Call for H.F.R.I. Research Projects to support Faculty members and Researchers and the procurement of high-cost research equipment grant" (Project Number: 1087, Acronym: SOL-art).

This book contains the compilation of works contributed to the *7th International Seminar on Organic Rankine Cycle Power Systems* (ORC 2023), held in Seville between the 4th and 6th of September 2023. The event was hosted by Universidad de Sevilla on behalf of the Knowledge Centre on Organic Rankine Cycle Technology (KCORC), incorporated in The Netherlands.

The ORC conference, organized biennially, stems as the only conference that is specific to ORC technology, therefore gathering a diverse community whose affiliation spans across all the interested stakeholders, not only in this particular technology but also and in a broader context, in the energy transition. Original equipment manufacturers, professional associations, end-users, investors, policy makers, academics, scientists feel at home at ORC 2023.

The almost 100 proceedings in this book cover a wide variety of topics, from fundamentals to system integration through component design, accounting for thermodynamic performance as well as component design. In addition to this, and as a new track in 2023, works on heat pump technology were also accepted in order to raise awareness of the strong ties between both technologies, specifically in energy storage applications.

This book provides an excellent overview of the current maturity of power systems based on Organic Rankine Cycle technology for applications as diverse as geothermal and waste heat recovery in industry or downstream of other prime movers (e.g., marine applications). It is also an excellent source of information to understand the current challenges faced by the technology, stemming from a very competitive market and increasingly stringent environmental regulations.

The organizers of ORC 2023 hope that the reader finds this work as exciting as the attendees to the conference and, maybe, make the decision to join the 8th edition to the conference in 2025.

KCORC
KNOWLEDGE CENTER
ORGANIC RANKINE CYCLE

eus EDITORIAL
UNIVERSIDAD DE SEVILLA